Superconducting diode effect in quasi-one-dimensional systems

Tatiana de Picoli,[1] Zane Blood,[2] Yuli Lyanda-Geller,[1] and Jukka I. Väyrynen[1]
[1]*Department of Physics and Astronomy, Purdue University, West Lafayette, Indiana 47907, USA*
[2]*Department of Physics, Cornell University, Ithaca, New York 14850, USA*

(Received 17 February 2023; revised 24 May 2023; accepted 12 June 2023; published 28 June 2023)

The recent observations of the superconducting diode effect pose the challenge to fully understand the necessary ingredients for nonreciprocal phenomena in superconductors. In this theoretical work, we focus on the nonreciprocity of the critical current in a quasi-one-dimensional superconductor. We define the critical current as the value of the supercurrent at which the quasiparticle excitation gap closes (depairing). Once the critical current is exceeded, the quasiparticles can exchange energy with the superconducting condensate, giving rise to dissipation. Our minimal model can be microscopically derived as a low-energy limit of a Rashba spin-orbit coupled superconductor in a Zeeman field. Within the proposed model, we explore the nature of the nonreciprocal effects of the critical current both analytically and numerically. Our results quantify how system parameters such as spin-orbit coupling and quantum confinement affect the strength of the superconducting diode effect. Our theory provides a complementary description to Ginzburg-Landau theories of the effect.

DOI: 10.1103/PhysRevB.107.224518

I. INTRODUCTION

Since their discovery, diodes have played an important role in the development of new technologies. Recently, the observation of nonreciprocity in the critical current of superconductors, known as the superconducting diode effect (SDE) [1–3], has brought attention to this phenomenon for its potential to achieve dissipationless electronics. Following the initial observations, extensive work has been done to show the signature of SDE in different bulk materials [4–8]. This diode effect was also observed and thoroughly studied in Josephson junctions [9–16] (first in the context of the anomalous Josephson effect [17–22]) and even in the absence of an applied magnetic field [23–27].

In general, nonreciprocity of the critical current occurs due to a broken inversion symmetry, which can be accomplished by an extrinsic or intrinsic mechanism. The first refers to the geometry of the system, the canonical example being an asymmetric superconducting ring threaded by a magnetic flux [7,28]. The SDE can also occur due to an intrinsic mechanism, for example, when one breaks the inversion of symmetry with spin-orbit coupling (SOC) [29–34]. However, experimentally it can be a challenge to determine whether the nonreciprocity comes strictly from the intrinsic features of the system [7]. Even theoretically, the exact minimal requirements for an intrinsic SDE remain unclear [35,36]. Most previous theoretical studies of intrinsic SDE have focused on using phenomenological Ginzburg-Landau theory (GL) [29,32,37–39], which is valid near the critical temperature $T \approx T_c$. While microscopic studies of the phenomenon have been conducted on two- and three-dimensional (2D and 3D) systems [29–34,38], a description of one-dimensional (1D) or quasi-1D systems has received less attention. The relative simplicity of 1D systems allows us to develop an analytical understanding of the problem.

In this paper, we present a Bogoliubov–de Gennes model that describes the main mechanisms to achieve the intrinsic diode effect in uniform 1D superconductors. In the 1D single-band regime, time-reversal invariant electronic systems can be generally described by a Hamiltonian of two helical bands with opposite helicities. We show that unequal Fermi velocities of the two helical bands generically lead to the SDE [see Fig. 1(a)]. Microscopically, we show that this happens in Rashba systems under quantum confinement or applied perpendicular magnetic field. Generally, an applied supercurrent can be written as $I_S = \rho_s \hbar q$ where $\rho_s = en/2m$ is the superfluid stiffness (in terms of the 1D superfluid density n and mass m) and $\hbar q$ is the Cooper pair momentum [40,41]. At low temperatures, when the superfluid density does not get appreciably modified by supercurrent, the study of nonreciprocity of the critical current $I_c = \rho_s q_c$ can be accomplished by calculating the critical momentum q_c by using the Cooper pair depairing condition [38,40–42] (we set $\hbar = k_B = 1$ hereon). Focusing here on s-wave pairing, each helical band (labeled by i) can be treated independently and has a superconducting gap Δ_i at the Fermi level. Qualitatively, Landau's criteria [43] in the absence of magnetic field gives $q_{ci} = \Delta_i / v_{Fi}$ for the ith helical band; the critical momentum of the system is then $q_c = \min_i\{q_{ci}\}$. For two bands with opposite helicities, applying a magnetic field B_z along the spin quantization axis will lower one q_{ci} while increasing the other [see Eq. (4)]. Even with equal gaps, $\Delta_1 = \Delta_2$, if the two bands have unequal Fermi velocities $v_{F1} \neq v_{F2}$, their critical momenta will become equal at a nonzero magnetic field $B_z = B_{z,0}$, leading to nonreciprocity. This behavior is shown in Figs. 1(b) and 1(c). For pairing $\Delta_i = \Delta$, the nonreciprocal behavior of the critical current, determined by the critical momentum, is fully explained by the difference of Fermi velocities, which carries information about inversion symmetry breaking.

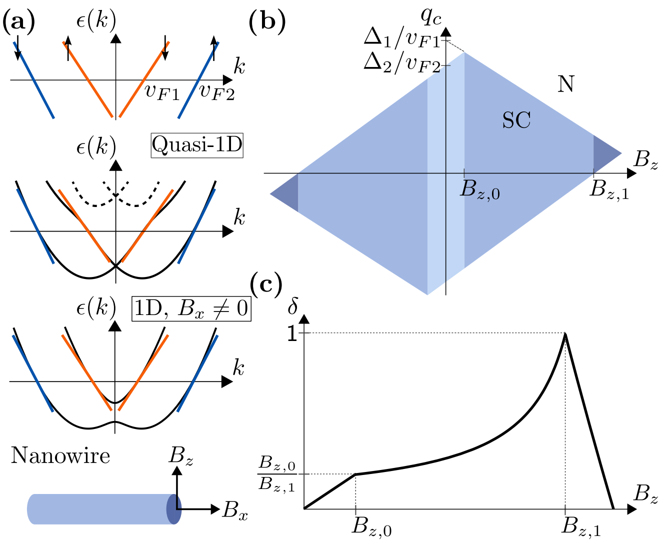

FIG. 1. (a) Top: Linearized energy spectrum in the normal state, showing two helical bands with unequal Fermi velocities and opposite helicities. The linearized model captures the Fermi level physics of quasi-1D and 1D Rashba models (bottom). In the quasi-1D case, hybridization between the lower (solid) and upper (dashed) Rashba bands leads to unequal Fermi velocities. In the purely 1D case the same can be achieved by applying a magnetic field B_x along the wire. (b) Phase diagram of the superconducting (SC) and normal (N) state determined by the critical momentum q_c as a function of the magnetic field B_z. The values of the magnetic field $B_{z,0}$ and $B_{z,1}$ delimit three different regions of the phase diagram. (c) Quality factor δ vs magnetic field B_z for the phase diagram shown in (b). The three regions of the phase diagram result in three different behaviors for the quality factor function.

II. LOW-ENERGY MODEL

To investigate the mechanisms responsible for the appearance of an intrinsic nonreciprocal behavior of the critical current, we investigate a low-energy minimal model. We propose a Hamiltonian of two helical bands,

$$H = \frac{1}{2}\sum_k C_k^\dagger \mathcal{H}_{\rm BdG} C_k, \tag{1}$$

where C_k is an eight-component Nambu spinor defined by $C_k = (C_{k1}\, C_{k2})^T$ with $C_{ki} = (c_{k+qi\uparrow}\, c_{k+qi\downarrow}\, c^\dagger_{-k+qi\downarrow}\, - c^\dagger_{-k+qi\uparrow})^T$. In this representation, $\uparrow, \downarrow$ are spins (or pseudospins) of our system and the subscript i is the label for each helical band. The Bogoliubov–de Gennes (BdG) Hamiltonian is given by $\mathcal{H}_{\rm BdG} = \mathrm{diag}(\mathcal{H}_{k1}, \mathcal{H}_{k2})$ with $[\chi_i = -(-1)^i]$ and

$$\mathcal{H}_{ki} = v_{Fi}(\chi_i k\sigma_z - k_{Fi})\tau_z + \chi_i v_{Fi} q\sigma_z + \Delta_i\tau_x + \frac{g_i\mu_B}{2}\vec{B}\cdot\vec{\sigma}. \tag{2}$$

In this effective model, each helical band is allowed to have in general an independent Fermi velocity v_{Fi}, Fermi momentum k_{Fi}, s-wave (intraband) pairing gap Δ_i, and g factor g_i, while experiencing the same applied magnetic field $\vec{B}$ (μ_B denotes the Bohr magneton). We have linearized the dispersion, focusing on low energies near the Fermi surface [see Fig. 1(a)]. The Pauli matrices $\sigma_{x,y,z}$ and $\tau_{x,y,z}$ act on the spin and particle-hole spaces, respectively. The parameter q is the Cooper pair momentum of the superconductor and determined by the externally applied supercurrent. Considering proximity-induced superconductivity at low temperatures, we are able to relate the Cooper pair momentum q to the applied supercurrent as $q \propto I_S$ in the first approximation. The analysis of nonreciprocity of the critical current can be performed by studying the behavior of the critical Cooper pair momentum q_c as a function of applied magnetic field. Although the beyond-mean-field description of a 1D system would typically involve fluctuations that can alter the behavior of physical properties, we consider here the case of proximity-induced pairing from a high-symmetry 3D superconductor which effectively suppresses these fluctuations.

From the above Hamiltonian (2), we find the energy cost $E_{\sigma i}(k)$ to create an excited above-gap quasiparticle of spin $\sigma = \uparrow, \downarrow = +, -$ and momentum k in the band i. For an applied magnetic field $\vec{B} = B_z\hat{z}$, this energy becomes

$$E_{\sigma i}(k) = \sigma\left(\frac{g_i\mu_B}{2}B_z + \chi_i q v_{Fi}\right) + \sqrt{\Delta_i^2 + (k - \chi_i\sigma k_{Fi})^2 v_{Fi}^2}. \tag{3}$$

Assuming for the moment B_z and q such that this energy cost is positive, the excitation energy of a quasiparticle will be the smallest at the Fermi momentum k_{Fi}. This energy cost can increase or decrease by tuning the applied magnetic field B_z and momentum q.

The critical momentum q_c of the system is the specific momentum for which $E_{\sigma i}(k = \chi_i\sigma k_{Fi}) = 0$, i.e., there is no energy cost to create a quasiparticle excitation [42–44]. For an applied current larger than the critical one, we expect the system to be in the normal phase (N) instead of the superconducting one (SC). Therefore, we focus our description for $q \leqslant q_c$. From the dispersion (3) we find that the critical momentum for each helical band is a linear function of the magnetic field

$$q_{ci}^\pm = \frac{-\chi_i\frac{1}{2}g_i\mu_B B_z \pm \Delta_i}{v_{Fi}}, \tag{4}$$

where the superscript $\pm$ labels the direction of the applied supercurrent. The critical momentum of the two-band system is then $q_c^\pm = \pm\min_{i=1,2}|q_{ci}^\pm|$.

The nonreciprocal behavior occurs when, for a fixed magnetic field, the absolute value of the critical current is different in the positive and negative directions. In terms of the critical momentum the nonreciprocity condition translates to $|q_c^+| \neq |q_c^-|$. To better understand how the physical parameters contribute to the superconducting diode effect, we can define a quality factor of the critical current as

$$\delta = \frac{|q_c^+| - |q_c^-|}{|q_c^+| + |q_c^-|}. \tag{5}$$

The phase diagram in Fig. 1(b) shows the phase separation between the normal and superconducting phase determined by the four components of the critical momentum (4). We define by $B_{z,0}$ ($-B_{z,0}$) the magnetic field in which the critical momentum of different helical bands first cross, i.e., $q_{c1}^+ = q_{c2}^+$ ($q_{c1}^- = q_{c2}^-$). Another characteristic value is the magnetic field $B_{z,1}$ in which the critical momentum q_{ci}^- changes sign. Without loss of generality, we assume $\Delta_2/v_{F2} < \Delta_1/v_{F1}$. For this choice of parameters, the explicit forms of $B_{z,0}$ and $B_{z,1}$ are found to be

$$B_{z,0} = \frac{\bar{\Delta}_1\bar{v}_{F2} - \bar{\Delta}_2\bar{v}_{F1}}{\bar{v}_{F1} + \bar{v}_{F2}}, \quad B_{z,1} = \min\{\bar{\Delta}_1, \bar{\Delta}_2\}, \tag{6}$$

where we define $\bar{v}_{Fi} = v_{Fi}/(\frac{1}{2}g_i\mu_B)$, $\bar{\Delta}_i = \Delta_i/(\frac{1}{2}g_i\mu_B)$. In Fig. 1(c) we show the behavior of the quality factor as a function of the magnetic field when $0 < B_{z,0} < B_{z,1}$. In general, we have a linear increase in the quality factor for small magnetic field, i.e., $\delta = B_z/B_{z,1}$ for $|B_z| < |B_{z,0}|$. For a larger magnetic field, the behavior of the quality factor is dependent on the particular choice of parameters. For the particular case shown in Fig. 1(c), where $B_{z,0}/B_{z,1} \ll 1$, the quality factor can be approximated by

$$\delta \approx \frac{B_z}{|B_z|}\frac{B_{z,0}}{-|B_z| + B_{z,0} + B_{z,1}} \quad (B_{z,0} < |B_z| < B_{z,1}), \tag{7}$$

reaching its maximum value 1 at $B_{z,1}$ when $|q_c^-| = 0$. The critical current becomes reciprocal and the diode effect disappears in the limit $B_{z,0} \to 0$. In this limit, the quality factor (5) becomes ill defined at the critical field $B_z = B_{z,1}$, but for any $B_z < B_{z,1}$ such that $|B_{z,1} - B_z| \gg B_{z,0}$, Eq. (7) yields a quality factor that vanishes as $\delta \propto B_{z,0}$ in the reciprocal limit. The ratio $B_{z,0}/B_{z,1}$, when small, is a characteristic measure for a weak diode effect.

III. SELF-CONSISTENT GAP

So far we focused the analysis of the transition between the superconducting to normal phase only on the critical Cooper pair momentum q_c. One could argue that $|q| > |q_c|$ is not a sufficient condition to ensure that the system is in the normal phase, i.e., that superconductivity could survive even in a gapless system. To study the practicability of such gapless superconductivity, we calculate the pairing potential self-consistently [45]. We note that in a self-consistent study of the proximity between a wire and a 3D superconductor, fluctuations have a negligible impact, which justifies the BdG approach to our system. This calculation also allows us to extend the low-energy model described to finite temperature. For one helical band, i.e., choosing subsystem i of (2), the self-consistency consists of solving for $\Delta_i \equiv \Delta_i(q, T)$ the equation

$$1 = V_i\int_{-k_D}^{k_D}\frac{dk}{2\pi}\frac{1 - f[E_{\uparrow i}(k)] - f[E_{\downarrow i}(-k)]}{2\sqrt{\Delta_i^2(q,T) + (k - \chi_i k_{Fi})^2 v_{Fi}^2}}, \tag{8}$$

where $f[E_{\sigma i}(k)]$ is the Fermi-Dirac distribution, $E_{\sigma i}(k)$ is the dispersion (3) calculated at $B_z = 0$, V_i/v_{Fi} is the dimensionless pairing interaction strength, and k_D is the Debye wave vector, providing a UV cutoff.

In Fig. 2 we show $\Delta(q, T)$ versus the Cooper pair momentum q plot for different values of temperature, obtained by solving Eq. (8) numerically. For $T = 0$ we find that $\Delta(q, 0)$ is constant for the Cooper pair momentum q below the critical one. For $q > q_c$, Eq. (8) has no solution, showing that the critical momentum found, Eq. (4), is the correct threshold to determine the SC to N transition in our 1D helical model. A nonzero B_z will only shift q_{ci} linearly, as described by Eqs. (3) and (4).

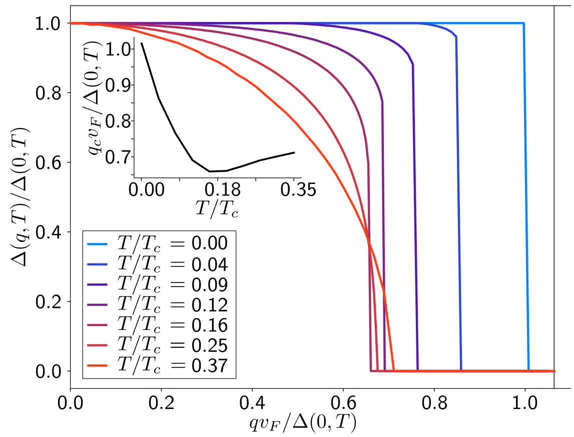

FIG. 2. Self-consistently calculated gap $\Delta(q, T)$ [in units of $\Delta(0, T)$] vs Cooper pair momentum q [in units of $\Delta(0, T)/v_F$]. Inset: The critical Cooper pair momentum $q_c(T)$ vs the temperature T normalized by $T_c = \Delta(0, 0)/(1.76k_B)$. Here, $q_c(T)$ is defined as the smallest q such that $\Delta(q, T) = 0$. This shows that at nonzero temperature, Eq. (4) can be approximately used with a temperature-dependent gap $\Delta(T)$ multiplied by a weakly temperature-dependent coefficient $q_c(T)/\Delta(0, T)$. The shown results are with $B_z = 0$; a nonzero B_z adds linearly to q [see Eq. (4)].

IV. MICROSCOPIC MODELS

Up to now, we have described an effective low-energy model that shows nonreciprocal phenomena and the mechanisms that allow the existence of the SDE. To complete our discussion, it is important to understand microscopically how to achieve unequal Fermi velocities between two helical bands. Here, we describe two Rashba systems that, in the low-energy limit, can be well described by our minimal model [46].

A. Quasi-1D Rashba wire

We start by considering a quasi-1D Rashba nanowire in the presence of a Zeeman field, described by the normal-state Hamiltonian [47],

$$H = \int dx\hat{\Psi}^\dagger(x)(\mathcal{H}_0 + \mathcal{H}_R + \mathcal{H}_Z)\hat{\Psi}(x), \tag{9}$$

with $\mathcal{H}_0 = -\frac{1}{2m}\partial_x^2 - \mu + E_0\Sigma_z$ and

$$\mathcal{H}_R = -i\alpha\partial_x\sigma_z + \eta\sigma_x\Sigma_y, \quad \mathcal{H}_Z = \tfrac{1}{2}g\mu_B\vec{B}\cdot\vec{\sigma}, \tag{10}$$

where $\hat{\Psi}(x) = [\hat{\psi}_{1\uparrow}(x) \quad \hat{\psi}_{1\downarrow}(x) \quad \hat{\psi}_{2\uparrow}(x) \quad \hat{\psi}_{2\downarrow}(x)]^T$ and $\Sigma_{x,y,z}$ are Pauli matrices that act on the transverse degree of freedom. Here, we consider the two lowest-energy transverse modes labeled by $i = 1, 2$. The Hamiltonian $\mathcal{H}_0$ describes the kinetic energy and confinement gap $2E_0 \propto 1/W^2$ between transverse bands. The Rashba Hamiltonian $\mathcal{H}_R$ is written in terms of α and $\eta \propto 1/W$ denoting the spin-orbit couplings respectively along and perpendicular to the wire. The parameters η and E_0 depend on the width W of the wire and the specific confining potential (see Ref. [48]). Our analysis, however, is completely independent regarding the specific forms of these parameters.

We first analyze $\mathcal{H}_0 + \mathcal{H}_R$ for the range of energy where only the lowest-energy transverse channel is occupied. This Hamiltonian commutes with the pseudospin operator $\sigma_z \Sigma_z$, therefore it is convenient to label the energies with $\sigma_z \Sigma_z$ eigenvalues ± 1. The dispersion of the lowest transverse mode is given by

$$\epsilon_\pm(k) = \frac{k^2}{2m} - \mu - \sqrt{(E_0 \pm \alpha k)^2 + \eta^2}. \quad (11)$$

From the dispersion, we find two positive Fermi momenta, $k_{F1,2}$, where k_{Fi} obeys $\epsilon_\pm(k_{Fi}) = 0$. We also find the Fermi velocities

$$v_{Fi} = \frac{k_{Fi}}{m} - \frac{\alpha(\alpha k_{Fi} \pm E_0)}{\sqrt{(\alpha k_{Fi} \pm E_0)^2 + \eta^2}}, \quad (12)$$

around k_{F1} $(-)$ and k_{F2} $(+)$.

In order to study the effects of weak magnetic field and proximity-induced superconductivity near the Fermi momenta, we linearize the dispersion by writing the field operator $\hat{\Psi}(x)$ as a superposition of left and right movers for each pseudospin subband,

$$\begin{aligned}\hat{\Psi}(x) = {}& [\hat{\psi}_{R\uparrow}(x)\sigma_x e^{ik_{F1}x} + \hat{\psi}_{L\downarrow}(x)e^{-ik_{F1}x}]\phi_1 \\ & + [\hat{\psi}_{R\downarrow}(x)e^{ik_{F2}x} + \hat{\psi}_{L\uparrow}(x)\sigma_x e^{-ik_{F2}x}]\phi_2, \end{aligned} \quad (13)$$

where $\phi_i = (i\sin\frac{\theta_i}{2}\ 0\ 0\ \cos\frac{\theta_i}{2})^T$ and $\theta_i = \arccos[\pm\alpha^{-1}(v_{Fi} - k_{Fi}/m)]$ with $+, -$ for $i = 1, 2$, respectively. We apply (13) to the Hamiltonian (9) for $\vec{B} = B_z\hat{z}$ to obtain an effective model for the quasi-1D nanowire in a perpendicular magnetic field. To obtain the low-energy description near the Fermi points, we assume that the components $\psi_{R(L)\sigma}(x)$ vary slowly in space allowing us to neglect terms $\partial_x^2\psi_{R(L)\sigma}(x)$. Likewise, fast oscillating terms $\propto e^{\pm i(k_{Fi}+k_{Fj})x}$ are also neglected [49]. We find the linearized dispersion of the nanowire in the normal phase,

$$\epsilon_{\sigma i}(k) = \sigma v_{Fi}(k - \sigma\chi_i k_{Fi}) + \sigma\frac{g_i\mu_B}{2}B_z, \quad (14)$$

where $g_i = g\cos\theta_i$. Finally, we include proximity-induced superconductivity with intrachannel pairing $\Delta e^{-2iqx}\sum_{i=1}^2 \hat{\psi}_{i\uparrow}\hat{\psi}_{i\downarrow}$ with Cooper pair momentum q. Linearizing the pairing term by substituting (13) into it, we are able to write the quasi-1D Rashba system using our minimal model Hamiltonian (2). Here, we find induced gaps $\Delta_1 = \Delta_2 = \Delta$ at the two Fermi momenta $k_{F1,2}$, respectively.

To understand the behavior of the quality factor δ in the quasi-1D case, we consider the limit $E_0 \gg \alpha^2 m, \eta, \mu$. In this regime, the energy difference between transverse bands is large, so the upper bands are unoccupied, but the hybridization η of the bands will change the Fermi velocities $v_{F1,2}$ by a small factor. To show the effects of small transverse coupling we expand the velocities v_{Fi} and g factor g_i in powers of η. Plugging this expansion into the expression for $B_{z,0}$ given by Eq. (6), we find $B_{z,0} \approx 2(m\alpha^2\eta^2/E_0^3)(\alpha/v_F)B_{z,1}$ and $B_{z,1} \approx \Delta/(\frac{1}{2}g\mu_B)$, where $v_F = \sqrt{2E_0/m}$. Thus, nonreciprocity arises in high order in spin-orbit coupling, stemming from weak hybridization of the transverse modes [46].

B. Purely 1D Rashba wire with B_x

As seen above, in the purely 1D model ($W \to 0, E_0 \to \infty$), the critical current becomes reciprocal ($B_{z,0} \to 0$). However, even in this case we can induce nonreciprocity by applying a transverse magnetic field which will lead to unequal velocities of the inner and outer Rashba modes [see Fig. 1(a)].

In the 1D limit the energy splitting E_0 between transverse bands is large and we can project the Hamiltonian Eq. (9) to the states with $\Sigma_z = -1$. Now the Hamiltonian commutes with σ_z (eigenvalues $\sigma = \pm 1$) and the energy dispersion gives equal Fermi velocities $v_F = \sqrt{2\mu/m + \alpha^2}$ for the inner and outer Rashba modes [50]. In this case, there is no nonreciprocity [51]. Next, we consider an additional component of the magnetic field in Eq. (10) as $B_x\sigma_x$, that acts in a similar way to the coupling η by breaking the conservation of spin [52]. To understand how the transverse magnetic field changes the velocities of the helical bands, we will treat this term perturbatively in the superconducting phase. First, we note that in the normal phase, the transverse magnetic field opens a gap at $k = 0$, affecting the inner helical band with smaller Fermi momentum $[k_{F1} = (v_F - \alpha)m]$ while presenting a negligible effect on the outer helical band with k_{F2}, as long as $\frac{1}{2}g\mu_B B_x \ll m\alpha v_F$. In the presence of proximity-induced superconductivity, the helical band around $k = k_{F1}$ (and similarly for $k = -k_{F1}$) can be described as $\mathcal{H}_{k1} = \mathrm{diag}(h_{k\uparrow}, h_{k\downarrow})$, where $h_{k\uparrow} = B_z + qv_{F1} + \Delta\tau_x$ and $h_{k\downarrow} \approx -2v_{F1}k_{F1}\tau_z$. By finding the eigenstates in the proximity of the Fermi level $\pm k_{F1}$, we can calculate the energy correction due to the applied perturbation B_x. We find $g_1 = g + \delta g$ and $v_{F1} = v_F + \delta v_F$, where $\frac{\delta v_F}{v_F} = \frac{\delta g}{g} = -(\frac{1}{4}\frac{g\mu_B B_x}{k_{F1}v_F})^2$, resulting in $v_{F2} > v_{F1}$, $g_2 > g_1$, and $\Delta_1 = \Delta_2$, thus leading to nonreciprocal critical current. In this case, we find $B_{z,0} \approx \frac{1}{2}(\frac{1}{4}\frac{g\mu_B B_x}{k_{F1}v_F})^2 B_{z,1}$ while $B_{z,1} \approx \Delta/(\frac{1}{2}g\mu_B)$, which implies the behavior of the quality factor as seen in Fig. 1(c).

V. DISCUSSION

We showed that helical bands with a Fermi velocity difference δv_F give rise to critical current nonreciprocity with the size of the effect quantified by $B_{z,0}/B_{z,1} \approx \delta v_F/v_F$ [see below Eq. (7)]. This form shows that the intrinsic superconducting diode effect is generally small in ordinary metals: The denominator is the Fermi velocity which increases with electron density whereas the numerator is the difference of Fermi velocities and typically (at most) of the order of the spin-orbit velocity, independent of the density.

In a quasi-1D system of width W, we found that $\delta v_F \sim \alpha m\alpha^2\eta^2/E_0^3$ arises from a transverse spin-orbit coupling $\eta \sim \alpha/W$. Since $E_0 \sim 1/(m_\perp W^2)$, we see that $\delta v_F \propto (W/l_\alpha)^4$ increases with the width of the system. Here, we introduced the Rashba length $l_\alpha = 1/(m\alpha)$ and assumed an isotropic effective mass $m_\perp \approx m$. This quasi-1D result is valid in the limit of small width, $W \ll l_\alpha$. The opposite limit of large W/l_α, is for general chemical potentials a complex problem due to multiple bands and Fermi points. Nevertheless, in the low-density case $\mu \ll m\alpha^2$ there are only two Fermi points, and we obtain a simple result $\delta v_F \sim \alpha E_0/(m\alpha^2) \propto (l_\alpha/W)^2$ by treating E_0 perturbatively. Thus, in low-density, clean, Rashba wires the nonreciprocity is a nonmonotonic function of the wire width, with a maximum at W of order the Rashba spin-orbit length, estimated to be of order 100 nm [53–56]. We emphasize however that this simple consideration is only valid in the low-density single-band regime and ignores disorder, Dresselhaus spin-orbit coupling, and mass anisotropies. Recently, in Ref. [57] it was observed that SDE is maximal at intermediate widths, although it is unclear if the effect stems from the same mechanism as we have outlined here.

In this paper we mostly focused on proximity-induced superconductivity in a semiconductor nanowire with low electron density. As a result, the nanowire is expected to determine the critical current of the entire system, allowing us to use an effective single-component model. Future studies of coupled systems could be performed using bosonization [58]. Additional research is needed to make quantitative predictions for optimizing the strength of intrinsic nonreciprocity in Rashba systems.

ACKNOWLEDGMENTS

We thank Leonid Rokhinson and Ananthesh Sundaresh for a related collaboration and discussions, and Leonid Glazman for valuable remarks. T.d.P. acknowledges the Graduate School for support under the Ross Fellowship Program. Z.B. was supported by NSF REU Grant No. PHY-1852501 and the ALPHA collaboration. This material is based upon work supported by the US Department of Energy, Office of Basic Energy Sciences, Division of Materials Sciences and Engineering under Award No. DE-SC0010544 (Y.L.-G.) and by the Office of the Under Secretary of Defense for Research and Engineering under Award No. FA9550-22-1-0354 (J.I.V.). This work was performed in part at Aspen Center for Physics, which is supported by National Science Foundation Grant No. PHY-1607611.

[1] S. A. Harrington, J. L. MacManus-Driscoll, and J. H. Durrell, Practical vortex diodes from pinning enhanced $YBa_2Cu_3O_{7-\delta}$, Appl. Phys. Lett. **95**, 022518 (2009).

[2] D. Y. Vodolazov, A. Y. Aladyshkin, E. E. Pestov, S. N. Vdovichev, S. S. Ustavshikov, M. Y. Levichev, A. V. Putilov, P. A. Yunin, A. I. El'kina, N. N. Bukharov *et al.*, Peculiar superconducting properties of a thin film superconductor–normal metal bilayer with large ratio of resistivities, Supercond. Sci. Technol. **31**, 115004 (2018).

[3] F. Ando, Y. Miyasaka, T. Li, J. Ishizuka, T. Arakawa, Y. Shiota, T. Moriyama, Y. Yanase, and T. Ono, Observation of superconducting diode effect, Nature (London) **584**, 373 (2020).

[4] R. Wakatsuki, Y. Saito, S. Hoshino, Y. M. Itahashi, T. Ideue, M. Ezawa, Y. Iwasa, and N. Nagaosa, Nonreciprocal charge transport in noncentrosymmetric superconductors, Sci. Adv. **3**, e1602390 (2017).

[5] R. Wakatsuki and N. Nagaosa, Nonreciprocal Current in Noncentrosymmetric Rashba Superconductors, Phys. Rev. Lett. **121**, 026601 (2018).

[6] Y. Hou, F. Nichele, H. Chi, A. Lodesani, Y. Wu, M. F. Ritter, D. Z. Haxell, M. Davydova, S. Ilić, O. Glezakou-Elbert, A. Varambally, F. S. Bergeret, A. Kamra, L. Fu, P. A. Lee, and J. S. Moodera, Ubiquitous superconducting diode effect in superconductor thin films, arXiv:2205.09276.

[7] A. Sundaresh, J. Ilmari Vayrynen, Y. Lyanda-Geller, and L. P. Rokhinson, Diamagnetic mechanism of critical current nonreciprocity in multilayered superconductors, Nat. Commun. **14**, 1628 (2023).

[8] L. Bauriedl, C. Bäuml, L. Fuchs, C. Baumgartner, N. Paulik, J. M. Bauer, K.-Q. Lin, J. M. Lupton, T. Taniguchi, K. Watanabe *et al.*, Supercurrent diode effect and magnetochiral anisotropy in few-layer $NbSe_2$, Nat. Commun. **13**, 4266 (2022).

[9] C.-Z. Chen, J. J. He, M. N. Ali, G.-H. Lee, K. C. Fong, and K. T. Law, Asymmetric Josephson effect in inversion symmetry breaking topological materials, Phys. Rev. B **98**, 075430 (2018).

[10] J. Diez-Merida, A. Díez-Carlón, S. Y. Yang, Y.-M. Xie, X.-J. Gao, K. Watanabe, T. Taniguchi, X. Lu, K. T. Law, and D. K. Efetov, Magnetic Josephson junctions and superconducting diodes in magic angle twisted bilayer graphene, arXiv:2110.01067.

[11] C. Baumgartner, L. Fuchs, A. Costa, S. Reinhardt, S. Gronin, G. C. Gardner, T. Lindemann, M. J. Manfra, P. E. Faria Junior, D. Kochan *et al.*, Supercurrent rectification and magnetochiral effects in symmetric Josephson junctions, Nat. Nanotechnol. **17**, 39 (2022).

[12] G. P. Mazur, N. van Loo, D. van Driel, J. Y. Wang, G. Badawy, S. Gazibegovic, E. P. A. M Bakkers, and L. P. Kouwenhoven, The gate-tunable Josephson diode, arXiv:2211.14283.

[13] C. Baumgartner, L. Fuchs, A. Costa, J. Picó-Cortés, S. Reinhardt, S. Gronin, G. C. Gardner, T. Lindemann, M. J. Manfra, P. E. F. Junior *et al.*, Effect of Rashba and Dresselhaus spin-orbit coupling on supercurrent rectification and magnetochiral anisotropy of ballistic Josephson junctions, J. Phys.: Condens. Matter **34**, 154005 (2022).

[14] B. Lu, S. Ikegaya, P. Burset, Y. Tanaka, and N. Nagaosa, Josephson diode effect on the surface of topological insulators, arXiv:2211.10572.

[15] M. Davydova, S. Prembabu, and L. Fu, Universal Josephson diode effect, Sci. Adv. **8**, eabo0309 (2022).

[16] Y. Zhang, Y. Gu, P. Li, J. Hu, and K. Jiang, General Theory of Josephson Diodes, Phys. Rev. X **12**, 041013 (2022).

[17] T. Ojanen, Topological π Josephson junction in superconducting Rashba wires, Phys. Rev. B **87**, 100506(R) (2013).

[18] F. Dolcini, M. Houzet, and J. S. Meyer, Topological Josephson ϕ_0 junctions, Phys. Rev. B **92**, 035428 (2015).

[19] K. N. Nesterov, M. Houzet, and J. S. Meyer, Anomalous Josephson effect in semiconducting nanowires as a signature of the topologically nontrivial phase, Phys. Rev. B **93**, 174502 (2016).

[20] M. Alidoust, C. Shen, and I. Žutić, Cubic spin-orbit coupling and anomalous Josephson effect in planar junctions, Phys. Rev. B **103**, L060503 (2021).

[21] J. Hasan, K. N. Nesterov, S. Li, M. Houzet, J. S. Meyer, and A. Levchenko, Anomalous Josephson effect in planar noncentrosymmetric superconducting devices, Phys. Rev. B **106**, 214518 (2022).

[22] A. Banerjee, M. Geier, M. Ahnaf Rahman, C. Thomas, T. Wang, M. J. Manfra, K. Flensberg, and C. M. Marcus, Phase asymmetry of Andreev spectra from Cooper-pair momentum, arXiv:2301.01881.

[23] J.-X. Lin, P. Siriviboon, H. D. Scammell, S. Liu, D. Rhodes, K. Watanabe, T. Taniguchi, J. Hone, M. S. Scheurer, and J. I. A. Li, Zero-field superconducting diode effect in small-twist-angle trilayer graphene, Nat. Phys. **18**, 1221 (2022).

[24] H. Wu, Y. Wang, Y. Xu, P. K. Sivakumar, C. Pasco, U. Filippozzi, S. S. P. Parkin, Y.-J. Zeng, T. McQueen, and M. N. Ali, The field-free Josephson diode in a van der Waals heterostructure, Nature (London) **604**, 653 (2022).

[25] T. H. Kokkeler, A. A. Golubov, and F. S. Bergeret, Field-free anomalous junction and superconducting diode effect in spin-split superconductor/topological insulator junctions, Phys. Rev. B **106**, 214504 (2022).

[26] H. D. Scammell, J. I. A. Li, and M. S. Scheurer, Theory of zero-field superconducting diode effect in twisted trilayer graphene, 2D Mater. **9**, 025027 (2022).

[27] J. Chiles, E. G. Arnault, C.-C. Chen, T. F. Q. Larson, L. Zhao, K. Watanabe, T. Taniguchi, F. Amet, and G. Finkelstein, Nonreciprocal supercurrents in a field-free graphene Josephson triode, Nano Lett. **23**, 5257 (2023).

[28] A. A. Burlakov, V. L. Gurtovoi, A. I. Il'in, A. V. Nikulov, and V. A. Tulin, Superconducting quantum interference device without Josephson junctions, JETP Lett. **99**, 169 (2014).

[29] N. F. Q. Yuan and L. Fu, Supercurrent diode effect and finite-momentum superconductors, Proc. Natl. Acad. Sci. USA **119**, e2119548119 (2022).

[30] S. Ilić and F. S. Bergeret, Theory of the Supercurrent Diode Effect in Rashba Superconductors with Arbitrary Disorder, Phys. Rev. Lett. **128**, 177001 (2022).

[31] K. Halterman, M. Alidoust, R. Smith, and S. Starr, Supercurrent diode effect, spin torques, and robust zero-energy peak in planar half-metallic trilayers, Phys. Rev. B **105**, 104508 (2022).

[32] A. Daido and Y. Yanase, Superconducting diode effect and nonreciprocal transition lines, Phys. Rev. B **106**, 205206 (2022).

[33] T. Karabassov, I. V. Bobkova, A. A. Golubov, and A. S. Vasenko, Hybrid helical state and superconducting diode effect in superconductor/ferromagnet/topological insulator heterostructures, Phys. Rev. B **106**, 224509 (2022).

[34] H. F. Legg, D. Loss, and J. Klinovaja, Superconducting diode effect due to magnetochiral anisotropy in topological insulators and Rashba nanowires, Phys. Rev. B **106**, 104501 (2022).

[35] D. F. Agterberg, Magnetoelectric effects, helical phases, and FFLO phases, in *Non-Centrosymmetric Superconductors: Introduction and Overview*, edited by E. Bauer and M. Sigrist (Springer, Berlin, Heidelberg, 2012), pp. 155–170.

[36] Y. Lyanda-Geller, J. I. Väyrynen, A. Sundaresh, and L. P. Rokhinson (unpublished).

[37] J. J. He, Y. Tanaka, and N. Nagaosa, A phenomenological theory of superconductor diodes, New J. Phys. **24**, 053014 (2022).

[38] A. Daido, Y. Ikeda, and Y. Yanase, Intrinsic Superconducting Diode Effect, Phys. Rev. Lett. **128**, 037001 (2022).

[39] D. Kochan, A. Costa, I. Zhumagulov, and I. Žutić, Phenomenological theory of the supercurrent diode effect: The Lifshitz invariant, arXiv:2303.11975.

[40] M. Tinkham, *Introduction to Superconductivity*, 2nd ed., Dover Books on Physics (Dover, New York, 2004).

[41] P. F. Bagwell, Critical current of a one-dimensional superconductor, Phys. Rev. B **49**, 6841 (1994).

[42] J. Bardeen, Critical fields and currents in superconductors, Rev. Mod. Phys. **34**, 667 (1962).

[43] L. Landau, Theory of the superfluidity of helium II, Phys. Rev. **60**, 356 (1941).

[44] V. L. Ginzburg and L. D. Landau, On the theory of superconductivity, in *On Superconductivity and Superfluidity* (Springer, Berlin, 2009), pp. 113–137.

[45] P.-G. de Gennes and P. A. Pincus, *Superconductivity of Metals and Alloys* (CRC Press, Boca Raton, FL, 2018).

[46] We expect similar physics in gate-defined wires in HgTe quantum wells [59].

[47] J. Alicea, New directions in the pursuit of majorana fermions in solid state systems, Rep. Prog. Phys. **75**, 076501 (2012).

[48] S. Park and A. L. Yeyati, Andreev spin qubits in multichannel Rashba nanowires, Phys. Rev. B **96**, 125416 (2017).

[49] B. van Heck, J. I. Väyrynen, and L. I. Glazman, Zeeman and spin-orbit effects in the Andreev spectra of nanowire junctions, Phys. Rev. B **96**, 075404 (2017).

[50] M. Houzet and J. S. Meyer, Quasiclassical theory of disordered Rashba superconductors, Phys. Rev. B **92**, 014509 (2015).

[51] The spin-orbit coupling can be gauged out in this case [60].

[52] T. Ojanen, Magnetoelectric Effects in Superconducting Nanowires with Rashba Spin-Orbit Coupling, Phys. Rev. Lett. **109**, 226804 (2012).

[53] A. E. Hansen, M. T. Björk, I. C. Fasth, C. Thelander, and L. Samuelson, Spin relaxation in InAs nanowires studied by tunable weak antilocalization, Phys. Rev. B **71**, 205328 (2005).

[54] C. Fasth, A. Fuhrer, L. Samuelson, V. N. Golovach, and D. Loss, Direct Measurement of the Spin-Orbit Interaction in a Two-Electron InAs Nanowire Quantum Dot, Phys. Rev. Lett. **98**, 266801 (2007).

[55] P. Roulleau, T. Choi, S. Riedi, T. Heinzel, I. Shorubalko, T. Ihn, and K. Ensslin, Suppression of weak antilocalization in InAs nanowires, Phys. Rev. B **81**, 155449 (2010).

[56] T. S. Jespersen, P. Krogstrup, A. M. Lunde, R. Tanta, T. Kanne, E. Johnson, and J. Nygård, Crystal orientation dependence of the spin-orbit coupling in InAs nanowires, Phys. Rev. B **97**, 041303(R) (2018).

[57] N. Satchell, P. M. Shepley, M. C. Rosamond, and G. Burnell, Supercurrent diode effect in thin film Nb tracks, J. Appl. Phys. **133**, 203901 (2023).

[58] C. Knapp, J. I. Väyrynen, and R. M. Lutchyn, Number-conserving analysis of measurement-based braiding with Majorana zero modes, Phys. Rev. B **101**, 125108 (2020).

[59] J. Reuther, J. Alicea, and A. Yacoby, Gate-Defined Wires in HgTe Quantum Wells: From Majorana Fermions to Spintronics, Phys. Rev. X **3**, 031011 (2013).

[60] Y. B. Lyanda-Geller and A. D. Mirlin, Novel Symmetry of a Random Matrix Ensemble: Partially Broken Spin Rotation Invariance, Phys. Rev. Lett. **72**, 1894 (1994).